VIP Polyhalogen Anions Very Important Paper

DOI: 10.1002/ange.201307552

An Adaptable and Dynamically Porous Organic Salt Traps Unique Tetrahalide Dianions**

Javier Martí-Rujas, Lorenzo Meazza, Gin Keat Lim, Giancarlo Terraneo, Tullio Pilati, Kenneth D. M. Harris, Pierangelo Metrangolo,* and Giuseppe Resnati**

Adaptable porous materials respond to guest species by undergoing dynamical structural changes on guest loading/loss. This behavior is reminiscent of proteins that respond to an external stimulus by conformational selection of an appropriate functional structure.[1] As an example of this new class of materials, a porous solid that combines preformed pores with the degrees of freedom of a peptide linker required for conformational selection has been described recently. This material displays adaptable porosity that evolves continuously from an open to a partially disordered closed structure in response to the level of guest loading.[2]

We have already demonstrated the dynamic behavior of α,ω-bis(trimethylammonium)alkane diiodides. These nonporous materials selectively take up α,ω-diiodoperfluoroalkanes[3] by gas–solid processes driven by the halogen bond (XB), the noncovalent interaction in which halogen atoms behave as electrophilic species (electron density acceptors, Lewis acids).[4] In these structures, the two iodide anions pin the α,ω-diiodoperfluoroalkane at each end by C–I···I⁻ XBs. Matching of the covalent N^+–N^+ separation in the dication with the separation of the iodide anions in the trimeric supramolecular dianion $I^-\cdots I-(CF_2)_n-I\cdots I^-$ controls the selectivity of the uptake process and effects the transformation of mismatching adducts into matching adducts. Similarly, when the diiodide salt **1a** of the 1,6-bis(trimethylammonium)hexane cation (hereafter the hexamethonium, $HMET^{2+}$, cation) reacts with one equivalent of I_2, the salt **3a** is formed.[5] Formation of the poorly stable,[6] halogen-bonded $[I_4]^{2-}$ dianion is favored both by size matching[7] of the interacting charged moieties (the N^+–N^+ and $I^-\cdots I^-$ separations in **3a** are 8.9 and 9.7 Å, respectively) and by a network of $I^-\cdots H-C$ short contacts, which drives an effective dimensional encapsulation of diiodine. **3a** is formed both from solution and from gas–solid reaction, demonstrating the dynamically porous character of bis(trimethylammonium)alkane diiodide salts. The ability of anions to work as effective XB acceptors is quite general as indicated by the diversity of the reported systems and the variety of associated functions, for example, transmembrane anion transport and organocatalysis.[8]

We show here that the series of bis(I_2) adducts [bis(trihalides)] **2a–c** of $HMET^{2+}\cdot 2X^-$ **1a–c** undergo thermally induced crystal-to-crystal elimination of one I_2 molecule resulting in quantitative formation of the virtually unknown tetrahalide species $[I_4]^{2-}$, $[I_2Br_2]^{2-}$, and $[I_2Cl_2]^{2-}$ (Scheme 1).[9,10] Short

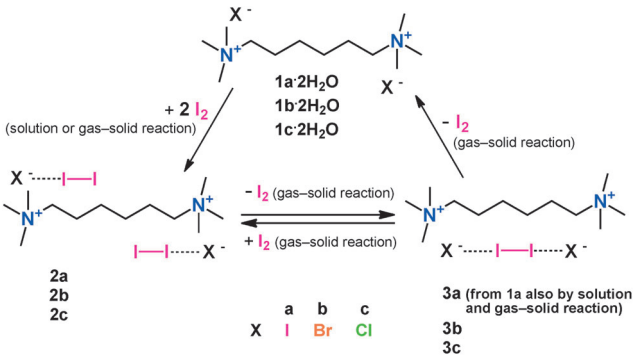

Scheme 1. Synthesis of tetrahalide dianions **3a–c** by thermally induced deiodination reactions of the bis(I_2) adducts **2a–c** and other interconversion reactions involving hexamethonium halides.

XBs to the halide anions result in double-pinning of a single I_2 molecule, and the tetrahalides obtained are selectively encaged by the $HMET^{2+}$ dications as a consequence of size-matching of the components and a network of cooperative anion···H–C short contacts. The starting materials **2a–c** are pre-organized in such a way to respond dynamically to heating, representing a functional structure that stabilizes the formation of the poorly stable tetrahalide species. In fact, **3b** and **3c** were never obtained in solution, proving that the confined environment of dynamically porous materials may confer unique and useful synthetic opportunities relative to solution-state processes.

When microcrystalline hexamethonium iodide **1a**, bromide **1b**, and chloride **1c** (used in their dihydrate forms) are

[*] Dr. J. Martí-Rujas
Italian Institute of Technology
Centre for Nano Science and Technology (CNST@PoliMi)
Via Pascoli 70/3, 20133 Milan (Italy)
Dr. L. Meazza, Dr. G. Terraneo, Dr. T. Pilati, Prof. Dr. P. Metrangolo, Prof. Dr. G. Resnati
NFMLab, D.C.M.I.C. "Giulio Natta", Politecnico di Milano
Via Mancinelli 7, 20131 Milan (Italy)
E-mail: pierangelo.metrangolo@polimi.it
giuseppe.resnati@polimi.it
Dr. G. K. Lim,[+] Prof. Dr. K. D. M. Harris
School of Chemistry, Cardiff University
Park Place, Cardiff, CF10 3AT, Wales (UK)
E-mail: HarrisKDM@cardiff.ac.uk
[+] Current address:
School of Chemical Sciences
Universiti Sains Malaysia, Pulau Pinang (Malaysia)

[**] This research was supported by Fondazione Cariplo (grant number 2010-1351) and MIUR (projects PRIN 2010–2011 grant numbers 2010CX2TLM_004 and 2010ERFKXL_005).

Supporting information for this article is available on the WWW under http://dx.doi.org/10.1002/anie.201307552.

kept in a sealed glass jar with solid I_2 for 1–2 days at room temperature, the starting white powders absorb I_2 and turn orange to brown. If two equivalents of I_2 are employed, differential scanning calorimetry (DSC) and powder X-ray diffraction (XRD) analyses show that bis(I_2) adducts **2a–c** are formed quantitatively. The same products are also obtained in quantitative yield by evaporation of methanol solutions in which **1a–c** and I_2 are present in 1:2 ratio;[11] crystals suitable for single-crystal XRD analysis are formed under these conditions. When one equivalent of I_2 is employed under gas–solid conditions, DSC and powder XRD show that **1a** affords the tetraiodide dianion salt **3a** in quantitative yield,[5] whereas **1b** and **1c** form the bis(trihalides) **2b** and **2c**, respectively, with half of the starting materials **1b** and **1c** remaining unchanged. Similar results are obtained when hexamethonium halides **1a–c** and equimolar amounts of I_2 are crystallized from methanol solutions.

The bis(trihalides) **2a–c** are isostructural and the central position of each trihalide anion, namely X2 in $[X1\cdots X2{-}X3]^-$, is always occupied by iodine. The cations and anions are stacked into columnar domains and four cationic columns embrace an anionic twin column formed by stacking of trihalide dimers (Figure 1).

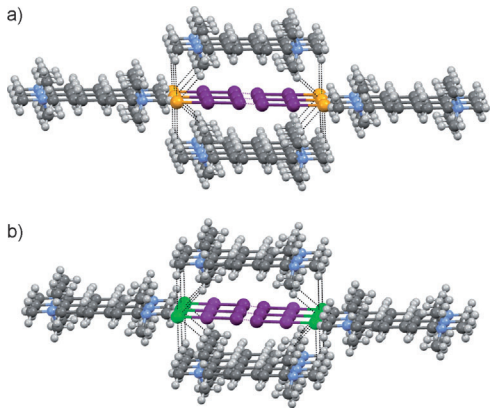

Figure 1. Ball-and-stick partial representation of: a) a column of $[I_2Br]^-$ dimers and bonded $HMET^{2+}$ cations in **2b** as obtained from single-crystal XRD analysis; b) a column of $[I_2Cl]^-$ dimers and bonded $HMET^{2+}$ cations in **2c** as obtained from single-crystal XRD analysis. $X^-\cdots H{-}C$ bonds and XBs are shown as black and magenta dashed lines, respectively. Color code: Light gray, hydrogen; dark gray, carbon; blue, nitrogen; brown, bromine; green, chlorine; violet, iodine.

$X^-\cdots H{-}C$ bonds (X = Cl, Br, I) play a decisive role in controlling the crystal packing of the bis(trihalides) **2a–c**. Twin columns of mixed trihalide anions $[X1\cdots X2{-}X3]^-$ are pinned in position by a network of $X^-\cdots H{-}C$ short contacts involving the trimethylammonium heads of the $HMET^{2+}$ cations and the outermost halogen atoms of the trihalide dimers.

Bromide and chloride anions tend to form stronger $X^-\cdots H{-}C$ bonds and electrostatic interactions than iodide anions, and in **2b,c** the mixed trihalide anions are oriented in order to maximize these interactions, that is, to position the bromine (**2b**) and chlorine (**2c**) atoms close to the trimethylammonium heads of the $HMET^{2+}$ cations. In all three crystal structures, the two outermost positions in the trihalide dimers are occupied by iodine (**2a**), bromine (**2b**), and chlorine (**2c**) atoms, and the two innermost positions are occupied by iodine atoms. In order to fit the columnar space identified by the four cationic columns, the innermost iodine atoms of the trihalide dimers are in close contact and give rise to type-I iodine···iodine contacts[12] with the typical sigmoidal arrangement. Type-I halogen···halogen contacts are polarization-driven interactions and iodine···iodine interactions are more favored than similar interactions involving bromine or chlorine atoms, and this also explains the orientation preferred by the mixed trihalides in the dimeric adducts **2b,c**.

α,ω-Bis(trimethylammonium)alkane dihalides[3] are nonporous materials by nature. The structure of anhydrous **1b** (determined from single-crystal XRD, see the Supporting Information) and its hydrate as well as of **1a,c**[10] confirm that this is also the case for our starting materials. The formation of **2a–c** from **1a–c** by solid–gas reactions described above proves the dynamic behavior of crystalline hexamethonium halides, but also reveals some limitations (under the conditions adopted) in the encapsulating ability of the $HMET^{2+}$ cation and its tendency to selectively pin a tetrahalide dianion, as **2b,c** are formed exclusively also when one equivalent of I_2 is used.

Thermally induced release of I_2 often occurs for solid polyiodides resulting in mixtures of adducts of various stoichiometries.[5] Under the hypothesis that, if one I_2 molecule is released from the bis(I_2) adducts **2**, the remaining four halogen atoms should be appropriately arranged to afford a tetrahalide dianion which is size-matched to the surrounding $HMET^{2+}$ cations, we investigated the thermally induced release of I_2 from **2**. As a consequence of the dynamically porous character of bis(trimethylammonium)alkane diiodide salts, we expected that the $HMET^{2+}$ cations may buffer the appreciable geometric changes that are anticipated to arise when one I_2 molecule is lost, by shrinking around the tetrahalide dianion formed and preserving the effective pinning of this anion through a network of $X^-\cdots H{-}C$ bonds similar to **2**. The double pinning of the same I_2 molecule by strong XBs to X^- and the formation of the networks of $X^-\cdots H{-}C$ contacts may promote the selective release of one of the two I_2 molecules present in the bis(I_2) adducts **2**. The isostructurality of **2a–c** should guarantee that the three adducts behave similarly.

Indeed, when powdered bis(triiodide) **2a** was slowly heated to 170 °C (heating rate 0.01 °C s^{-1}) in a closed chamber in the powder X-ray diffractometer, **2a** transformed quantitatively into **3a** in a crystal-to-crystal process. When the bis(diiodobromide) **2b** and the bis(diiodochloride) **2c** were heated under similar conditions, new crystalline solids appeared at about 100 °C and the reactions were complete at about 160 °C (Figure 2 and Figure S12). The new solids are stable at room temperature and in contact with air for over a week, and elemental analyses confirm that only one I_2 molecule is released (see the Experimental Section and the Supporting Information).

The crystallinity of organic materials is often found to decrease upon heating, resulting in ill-defined powder XRD patterns that do not allow the crystal structure to be

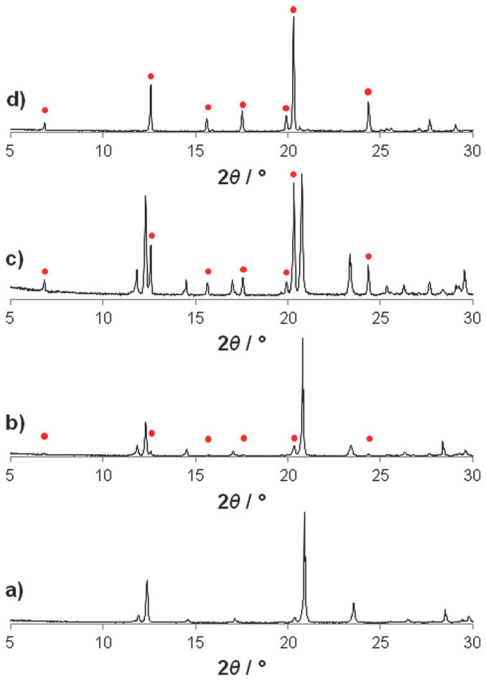

Figure 2. Powder XRD data recorded as a function of temperature starting from **2b**: a) only **2b** is observed at 50 °C; a mixture of **2b** and **3b** (red dots) is observed at b) 120 °C and c) 140 °C; d) only **3b** is observed at 160 °C.

determined by analysis of the powder XRD data. However, despite the high temperature required for their solid-state synthesis, the crystallinity of the new adducts obtained from **2a–c** is good (Figure 2d, and Figures S4, S12) and here we have determined the crystal structures of **3b** and **3c** directly from powder XRD data. Following successful indexing of the powder XRD patterns of **3b** and **3c**, the space groups were determined from systematic absences as *C2m* (the same as **3a**). Structure solution of **3b** was carried out directly from the powder XRD data using the direct-space genetic algorithm (GA) technique[13] (implemented in the program EAGER[14]), followed by Rietveld refinement (Figure 3). In the case of **3c**, the structure of **3b** was used as the starting point for Rietveld refinement (but with the Br atom replaced by Cl). The good

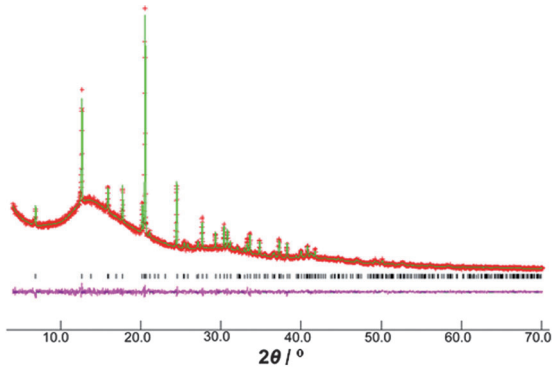

Figure 3. Final Rietveld refinement of **3b** from powder XRD data, showing the experimental (red + marks), calculated (green solid line), and difference (lower pink line) powder XRD profiles.

agreement between the experimental and calculated powder XRD patterns evident from the residual difference plots in the final Rietveld refinements of **3b** and **3c** corroborates the correctness of the structures (Figure 3 and Supporting Information).

As expected, the previously unknown $[I_2Br_2]^{2-}$ and the very rare $[I_2Cl_2]^{2-}$ tetrahalide anions are present as discrete species in **3b**,**c**, respectively (Figure 4). In each case, the lighter halogen atoms occupy the outer positions of the dianions and hold the I_2 molecules at each end through short and linear I–I···X^- (X = Br, Cl) XBs.

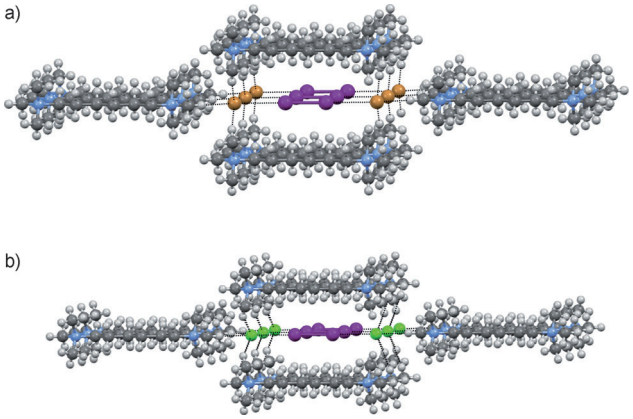

Figure 4. Ball-and-stick partial representation of a column of dianions a) $[I_2Br_2]^{2-}$ and b) $[I_2Cl_2]^{2-}$ along with bonded $HMET^{2+}$ cations in the crystal structures of **3b** and **3c**, respectively. X^-···H–C bonds and XBs are shown as black dashed lines, respectively. Color codes as in Figure 1.

The I–I···X^- distances are 339.7(8) and 317.0(8) pm (about 0.85 times the sum of the van der Waals radius of iodine and the Pauling ionic radius of the halide anion) and the I–I···X^- angles are 177.22(8)° and 175.74(8)° for $[I_2Br_2]^{2-}$ and $[I_2Cl_2]^{2-}$, respectively. Cation and anion size-matching is quite good; for instance, in **3b** the N^+–N^+ and Br^-···Br^- separations are 874.5 and 948.1 pm, respectively. As expected, the mixed tetrahalides $[I_2X_2]^{2-}$ are held in place by a network of X^-···H–C bonds similar to those in **2b**,**c**.

Thermogravimetric (TG) analysis and DSC are very useful for demonstrating that **3b**,**c** undergo a stepwise loss of I_2. For instance, DSC analysis of **2b** shows two endothermic peaks at 163.6 and 208.4 °C (Figure S8) corresponding to the melting points of the starting material **2b** and the product **3b** formed under DSC conditions, respectively. Interestingly, TG analysis demonstrates that the release of one I_2 molecule from **2b** starts at about 85 °C, namely well ahead of the melting, while release of the remaining I_2 molecule from **3b** occurs across its melting point (which starts at 188 °C and ends at 234 °C). Both **3a** and **3c** behave similarly. In particular, the first I_2 molecule is released from **2c** in the range 95–170 °C and the second from **3c** between 178–217 °C (the melting point of **2c** is 158 °C and that of **3c** is 202 °C). The fact that I_2 is released from **3a–c** only close to their melting points highlights the effective I_2 encapsulation by size-matching confinement that operates in these adducts. The importance of size

matching is further confirmed by the preparation and thermal analysis of three mismatched complexes, namely the bis(I_2) adducts of tetramethonium, octamethonium (see the Supporting Information), and dodecamethonium iodides,[15] for which I_2 is released in only one step across a wide range of temperatures.

The structures of **3a–c** do not possess permanent porosity. In fact, after annealing **3a–c** for 72 h at 170 °C in air, powder XRD confirms that the remaining I_2 molecule is lost and the materials revert to the dihydrate forms **1a–c**. The space created in **3a–c** on loss of I_2 is not sustained by the structure, water is absorbed from air and a different architecture is adopted, consistent again with the dynamic character of hexamethonium salts. Moreover, when microcrystalline **1a–c** thus obtained are exposed to I_2 vapor, the bis(trihalides) **2a–c** are re-formed, further demonstrating the dynamic behavior of hexamethonium salts. In general for polyiodides, as the iodine content increases, the material becomes darker and the melting point decreases. The diiododichloride **3c** is, in fact, ochre and melts at 209 °C, whereas the bis(diiodochloride) **2c** is brown (Figure 5) and melts at 164 °C. Similar changes in color and melting point are observed when **1a**,**b** adsorb I_2 to afford **2a**,**b** and when **2a**,**b** lose I_2 to afford **3a**,**b** (Figure S20).[5]

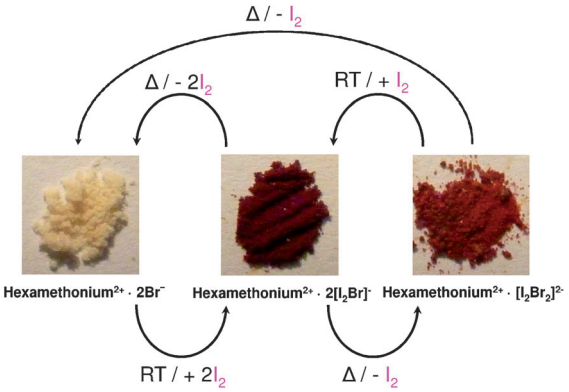

Figure 5. Photographs showing the color change observed on interconversion of hexamethonium bis(bromide) (**1b**, white, left), bis(diiodobromide) (**2b**, brown, center), and diiododibromide (**3b**, orange, right).

In conclusion, we have reported herein that thermal treatment of microcrystalline trihalides **2a–c** affords the $[I_4]^{2-}$ tetraiodide anion and its unique $[I_2Br_2]^{2-}$ and $[I_2Cl_2]^{2-}$ mixed analogs as uniform and microcrystalline hexamethonium salts **3a–c**. In the case of **3b** and **3c**, we have exploited the opportunities that now exist for determining the crystal structures of microcrystalline materials directly from powder XRD data. The discovery of new polyhalogen anions is a research topic of considerable interest.[16] Our results represent the first structural evidence of a discrete diiododibromide $[I_2Br_2]^{2-}$ anion, and only the second report of the $[I_2Cl_2]^{2-}$ anion. These novel anions are obtained upon thermally induced dynamic rearrangement of the starting materials **2a–c** as a result of size-matching induced stabilization. Interestingly, **3b** and **3c** could not be obtained from solution. This behavior is reminiscent of biological processes in which a substrate, located in an enzyme pocket, forms a product that is inaccessible under different conditions as a result of fact that the nearby enzymatic residues, preorganized around the substrate, easily adapt around the product to favor its formation through a network of stabilizing interactions. The power of cavity-directed reactivity in dynamic crystalline solids is fully proven and affords new opportunities for synthesis and interconversion of polyhalogen anions, a key process in some technologically relevant phenomena such as charge transfer in dye-sensitised solar cell (DSSC) electrolyte solutions.[17]

Experimental Section

Single-crystal XRD data for **2b**: $C_{12}H_{30}N_2^{2+}\cdot 2(BrI_2^-)$, $M_r = 869.80$, monoclinic, *C2m*, $a = 22.073(5)$, $b = 7.5014(14)$, $c = 7.3922(15)$ Å, $\beta = 92.195(8)°$, $V = 1223.1(4)$ Å^3, $T = 220(2)$ *K*, $Z = 2$, $\rho_{calcd} = 2.362$ g cm^{-3}, 9136 reflections measured, 1509 independent reflections, 64 parameters, 3 restraints, $2.87° < \theta < 27.48°$, R_1 $[I > 2\sigma(I)] = 0.0292$, and wR^2 $[I > 2\sigma(I)] = 0.0594$.

High-quality powder XRD data were recorded at ambient temperature on a Bruker D8 diffractometer (transmission mode; Ge-monochromated CuKα1; $\lambda = 1.5406$ Å; Vantec detector covering 12° in 2θ; 2θ range, 4–70°; step size, 0.017°; data collection time, 14 h). The high background observed in the powder XRD pattern is a consequence of carrying out data collection using a foil sample holder in transmission geometry.

Structure determination of **3b** from powder XRD data: the data were indexed using the program LZON[18] to give a monoclinic unit cell ($a = 25.84$, $b = 7.27$, $c = 5.59$ Å, $\beta = 93.6°$; $V = 1047.8$ Å^3). The space group was assigned from systematic absences as *C2m*. Unit cell and profile refinement, carried out using the Le Bail method,[19] gave an excellent fit ($R_{wp} = 3.25\,\%$, $R_p = 2.45\,\%$). Structure solution was carried out using the direct-space GA technique implemented in the program EAGER, followed by Rietveld refinement using the GSAS program. In the Rietveld refinement, standard restraints were applied to bond lengths and angles and isotropic displacement parameters were refined. Final Rietveld refinement: $a = 25.8309(10)$, $b = 7.26762(30)$, $c = 5.58438(27)$ Å, $\beta = 93.602(4)°$; $V = 1046.28(11)$ Å^3; $R_{wp} = 3.39\,\%$, $R_p = 2.55\,\%$; 3878 profile points; 98 refined variables.

Structure determination of **3c** from powder XRD data: the data were indexed using the program ITO[20] to give a monoclinic unit cell ($a = 26.08$, $b = 6.88$, $c = 5.65$ Å, $\beta = 95.5°$; $V = 1010.3$ Å^3). The space group was assigned from systematic absences as *C2m*. Profile fitting using the Le Bail method gave an excellent fit ($R_{wp} = 3.07\,\%$, $R_p = 2.34\,\%$). As the unit cell is very similar to that of **3b** and the space group is identical, the structure of **3b** was used as the starting point for Rietveld refinement of **3c**, but with Br replaced by Cl. Rietveld refinement was carried out as described above for **3b**. Final Rietveld refinement: $a = 26.0883(4)$, $b = 6.88603(10)$, $c = 5.65418(10)$ Å, $\beta = 95.5164(15)°$; $V = 1011.04(4)$ Å^3; $R_{wp} = 3.27\,\%$, $R_p = 2.46\,\%$; 3878 profile points; 98 refined variables.

CCDC 952026 (**2b**), 952028 (**3b**), 952029 (**3c**) contains the supplementary crystallographic data for this paper. These data can be obtained free of charge from The Cambridge Crystallographic Data Centre via www.ccdc.cam.ac.uk/data_request/cif. The Supporting Information contains additional crystallographic data and CCDC numbers for the bis(triiodide) of tetramethonium and the solvates and hydrates of hexamethonium halides.

Received: August 27, 2013
Published online: November 7, 2013

Keywords: halogen bonds · hydrogen bonds · polyhalogen anions · single crystals · X-ray diffraction

[1] D. D. Boehr, R. Nussinov, P. E. Wright, *Nat. Chem. Biol.* **2009**, *5*, 789 – 796.
[2] J. Rabone, Y.-F. Yue, S. Y. Chong, K. C. Stylianou, J. Bacsa, D. Bradshaw, G. R. Darling, N. G. Berry, Y. Z. Khimyak, A. Y. Ganin, P. Wiper, J. B. Claridge, M. J. Rosseinsky, *Science* **2010**, *329*, 1053 – 1057.
[3] P. Metrangolo, Y. Carcenac, M. Lahtinen, T. Pilati, K. Rissanen, A. Vij, G. Resnati, *Science* **2009**, *323*, 1461 – 1464.
[4] a) P. Metrangolo, H. Neukirch, T. Pilati, G. Resnati, *Acc. Chem. Res.* **2005**, *38*, 386 – 395; b) P. Metrangolo, F. Meyer, T. Pilati, G. Resnati, G. Terraneo, *Angew. Chem.* **2008**, *120*, 6206 – 6220; *Angew. Chem. Int. Ed.* **2008**, *47*, 6114 – 6127; c) G. R. Desiraju, P. S. Ho, L. Kloo, A. C. Legon, R. Marquardt, P. Metrangolo, P. A. Politzer, G. Resnati, K. Rissanen, *Pure Appl. Chem.* **2013**, *85*, 1711 – 1713.
[5] A. Abate, M. Brischetto, G. Cavallo, M. Lahtinen, P. Metrangolo, T. Pilati, S. Radice, G. Resnati, K. Rissanen, G. Terraneo, *Chem. Commun.* **2010**, *46*, 2724 – 2726.
[6] M. Müller, M. Albrecth, V. Gossen, T. Peters, A. Hoffmann, G. Raabe, A. Valkonen, K. Rissanen, *Chem. Eur. J.* **2010**, *16*, 12446 – 12453.
[7] a) M. I. Nelen, A. V. Eliseev, *J. Chem. Soc. Perkin Trans. 2* **1997**, 1359 – 1364; b) M. W. Hosseini, J. M. Lehn, *J. Am. Chem. Soc.* **1982**, *104*, 3525 – 3527.
[8] a) A. Vargas Jentzsch, D. Emery, J. Mareda, P. Metrangolo, G. Resnati, S. Matile, *Angew. Chem.* **2011**, *123*, 11879 – 11882; *Angew. Chem. Int. Ed.* **2011**, *50*, 11675 – 11678; b) F. Kniep, S. H. Jungbauer, Q. Zhang, S. M. Walter, S. Schindler, I. Schnapperelle, E. Herdtweck, S. M. Huber, *Angew. Chem.* **2013**, *125*, 7166 – 7170; *Angew. Chem. Int. Ed.* **2013**, *52*, 7028 – 7032.
[9] There are no structures in the Cambridge Structural Database (CSD) containing the discrete $[I_2Br_2]^{2-}$ dianion, whereas $[I_2Cl_2]^{2-}$ is found in only one structure (Ref. [10a]) and a few reports describe $[I_4]^{2-}$ (Ref. [6]) and $[Br_4]^{2-}$ (Refs. [10b,c]).
[10] a) I. E. Parigoridi, G. J. Corban, S. K. Hadjikakou, N. Hadjiliadis, N. Kourkoumelis, G. Kostakis, V. Psycharis, C. P. Raptopoulou, M. Kubicki, *Dalton Trans.* **2008**, 5159 – 5165; b) G. B. M. Vaughan, A. J. Mora, A. N. Fitch, P. N. Gates, A. S. Muir, *J. Chem. Soc. Dalton Trans.* **1999**, 79 – 84; c) M. C. Aragoni, M. Arca, F. A. Devillanova, M. B. Hursthouse, S. L. Huth, F. Isaia, V. Lippolis, A. Mancini, H. Ogilvie, *Inorg. Chem. Commun.* **2005**, *8*, 79 – 82.
[11] L. Meazza, J. Martí-Rujas, G. Terraneo, C. Castiglioni, A. Milani, T. Pilati, P. Metrangolo, G. Resnati, *CrystEngComm* **2011**, *13*, 4427 – 4435.
[12] G. R. Desiraju, R. Parthasarathy, *J. Am. Chem. Soc.* **1989**, *111*, 8725 – 8726.
[13] a) K. D. M. Harris, E. Y. Cheung, *Chem. Soc. Rev.* **2004**, *33*, 526 – 538; b) K. D. M. Harris, *Cryst. Growth Des.* **2003**, *3*, 887 – 895; c) K. D. M. Harris, M. Tremayne, B. Kariuki, *Angew. Chem.* **2001**, *113*, 1674 – 1700; *Angew. Chem. Int. Ed.* **2001**, *40*, 1626 – 1651; d) *Structure Determination from Powder Diffraction Data*, *Vol. 13* (Eds.: W. I. F. David, K. Shankland, L. B. McCusker, C. Baerlocher), OUP, Oxford, UK, **2002**.
[14] a) E. Tedesco, G. W. Turner, K. D. M. Harris, R. L. Johnston, B. M. Kariuki, *Angew. Chem.* **2000**, *112*, 4662 – 4665; *Angew. Chem. Int. Ed.* **2000**, *39*, 4488 – 4491; b) K. D. M. Harris, S. Habershon, E. Y. Cheung, R. L. Johnston, *Z. Kristallogr.* **2004**, *219*, 838 – 846.
[15] Unpublished results.
[16] H. Haller, J. Schröder, S. Riedel, *Angew. Chem.* **2013**, *125*, 5037 – 5040; *Angew. Chem. Int. Ed.* **2013**, *52*, 4937 – 4940.
[17] a) C. Teng, X. Yang, C. Yuan, C. Li, R. Chen, H. Tian, S. Li, A. Hagfeldt, L. Sun, *Org. Lett.* **2009**, *11*, 5542 – 5545; b) A. Abate, A. Petrozza, V. Roiati, S. Guarnera, H. Snaith, F. Matteucci, G. Lanzani, P. Metrangolo, G. Resnati, *Org. Electron.* **2012**, *13*, 2474 – 2478.
[18] R. Shirley, D. Louër, *Acta Crystallogr. Sect. A* **1978**, *34*, S382.
[19] A. Le Bail, H. Duroy, J. L. Fourquet, *Mater. Res. Bull.* **1988**, *23*, 447 – 572.
[20] J. W. Visser, *J. Appl. Crystallogr.* **1969**, *2*, 89 – 95.